J. Phys. A: Math. Gen. **30** (1997) 3817–3836. Printed in the UK PII: S0305-4470(97)79382-X

Asymmetric XXZ chain at the antiferromagnetic transition: spectra and partition functions

Doochul Kim

Department of Physics and Center for Theoretical Physics, Seoul National University, Seoul 151-742, South Korea

Received 8 November 1996

Abstract. The Bethe ansatz equation is solved to obtain analytically the leading finite-size correction of the spectra of the asymmetric XXZ chain and the accompanying isotropic 6-vertex model near the antiferromagnetic phase boundary at zero vertical field. The energy gaps scale with size N as $N^{-1/2}$ and their amplitudes are obtained in terms of level-dependent scaling functions. Exactly on the phase boundary, the amplitudes are proportional to a sum of square-root of integers and an anomaly term. By summing over all low-lying levels, the partition functions are obtained explicitly. A similar analysis is performed also at the phase boundary of zero horizontal field in which case the energy gaps scale as N^{-2}. The partition functions for this case are found to be that of a non-relativistic free fermion system. From the symmetry of the lattice model under $\pi/2$ rotation, several identities between the partition functions are found. The $N^{-1/2}$ scaling at zero vertical field is interpreted as a feature arising from viewing the Pokrovsky–Talapov transition with the space and time coordinates interchanged.

1. Introduction

Spectral properties of the asymmetric XXZ chain and its associated lattice model, the asymmetric 6-vertex model, have recently been of much interest [1–6]. The Hamiltonian of the asymmetric XXZ chain is displayed as equation (1) in the next section. It is a non-Hermitian generalization of the standard spin $\frac{1}{2}$ XXZ chain [7] and is the anisotropic limit of the row-to-row transfer matrix of the asymmetric 6-vertex model, i.e. the general 6-vertex model in horizontal and vertical fields [8–10]. Both models are solvable by the Bethe ansatz for arbitrary interaction parameter Δ, horizontal field H and vertical field V, and for the lattice model, also for the arbitrary anisotropy parameter.

When the interaction parameter Δ is less than -1, the asymmetric XXZ chain and the asymmetric 6-vertex model are antiferromagnetically ordered for small values of H and V. (We use the term antiferromagnetic phase to denote the antiferroelectric phase of the lattice model.) Typical phase diagrams in the H–V plane are shown in figure 1. The ordered phase in the H–V plane is bounded by the antiferromagnetic phase boundary, shown in figure 1 as the full curve, beyond which the systems are disordered. The disordered phase is critical in that excitations are massless and correlation lengths decay algebraically. For still larger values of fields, complete ferromagnetic ordering sets in. The free energy of the 6-vertex model as a function of the two fields can be interpreted as the equilibrium crystal shape [11-13] and the antiferromagnetically ordered region of fields corresponds to the flat facet, and the antiferromagnetic phase boundary to the facet boundary. On the facet boundary, the curvature of the free energy surface is universal [14, 3]. The nature of phase transitions

0305-4470/97/113817+20$19.50

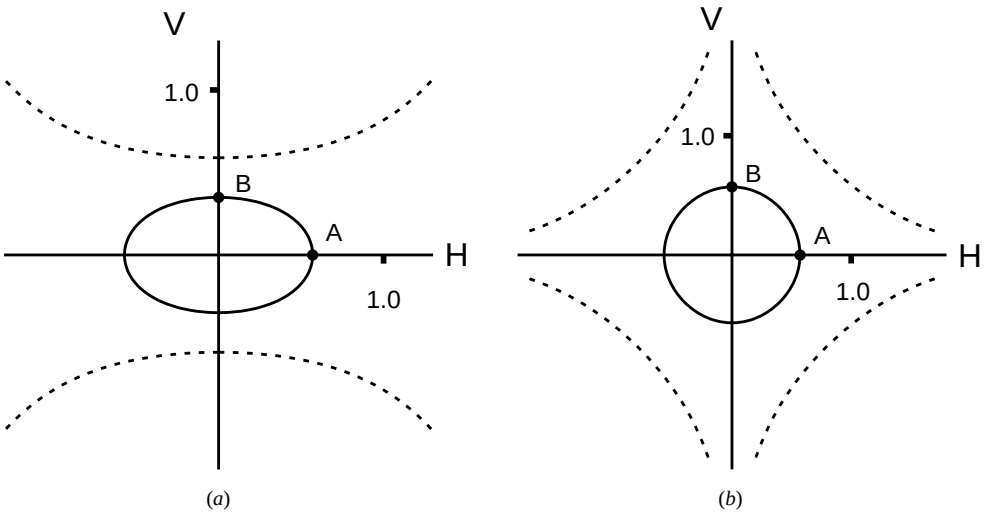

Figure 1. (*a*) Phase diagram in fields of the asymmetric XXZ chain for $\lambda = 2.5$. The full curve is the antiferromagnetic phase boundary and the broken ones are the ferromagnetic phase boundary. The region between the curves is the critical phase. The point A (B) is the $H = H_c$, $V = 0$ ($H = 0$, $V = V_c$) phase boundary discussed in section 5 (6). (*b*) The same as in (*a*) for the isotropic 6-vertex model (F model).

at the facet boundary can be understood from the viewpoint of domain wall excitations and is that of the Pokrovsky–Talapov (PT) transition [15, 16].

Within the critical phase and on the phase boundaries, an infinite number of massless excitations exists in the thermodynamic limit. When the system size, i.e. the number of spins in the chain N, is finite, the degeneracies are lifted producing energy gaps. Finite-size scaling of these energy gaps gives valuable information on the properties of the system [17]. Throughout the critical phase of the asymmetric XXZ chain and the asymmetric 6-vertex model, the energy gaps scale as N^{-1} and, as shown in [3], the finite-size scaling amplitudes can be accounted for by the central charge $c = 1$ conformal field theory [18], with suitable modifications to account for incommensurate arrow densities. All finite-size scaling information is encoded in the O(1) part of the partition function which is covariant under the modular transformations and, for the case of the asymmetric 6-vertex model, is given by the modified Coulombic partition function.

When $\Delta > 1$ and $V = 0$, the critical phase is bounded by the so-called stochastic line where the asymmetric XXZ chain Hamiltonian describes the time evolution of the single-step model [19] which is one of the simplest realizations of the Kardar–Parisi–Zhang (KPZ) universality class of non-equilibrium growth models [20] and also of the driven lattice gas [21, 22]. On the stochastic line, the N^{-1} scaling crossovers to the KPZ-type $N^{-3/2}$ scaling where the exponent $\frac{3}{2}$ is the dynamic exponent for the $(1+1)$-dimensional KPZ class. This was first shown in [4] for a special limit (see also [23]), and numerically in [5] for other cases. More recently, it was shown in [6], which will be denoted as I in this work, that the energy gaps for general cases can be systematically expanded in power series of $N^{-1/2}$ and the scaling amplitudes are given by level-dependent, but universal, scaling functions.

Recently, the finite-size scaling on the antiferromagnetic phase boundary of $V = 0$ was discussed by Albertini *et al* [1, 2]. In their work, it was shown analytically that the low-lying excitations satisfy the energy–momentum relation $\varepsilon \sim \sqrt{\mathrm{i}k}$ in the thermodynamic

limit which in turn indicates the $N^{-1/2}$ scaling of energy gaps. It was then confirmed by numerical solutions of the Bethe ansatz equations for finite N that the energy gaps scale as $N^{-1/2}$.

In this work, we present analytic solutions for the finite-size scaling at the antiferromagnetic phase boundary using the method developed in I. It is seen that the $N^{-1/2}$ scaling of energy gaps for $V = 0$ phase boundary arises from the same mathematical origin as in the case of the stochastic line. The scaling amplitudes for general levels are given in terms of a scaling variable $u \sim (H - H_c)N$ where H_c is the position of the phase boundary at $V = 0$. Their crossover behaviours enable one to identify the class of levels which become degenerate at the phase boundary of $|H| < H_c$. At $H = H_c$, the energy gap amplitudes are found to be proportional to a sum of square-root of integers and an anomaly term. Furthermore, the O(1) part of the partition function in the scaling limit, which is simply called the partition function in this work, is also obtained for both the chain and the lattice model in terms of several infinite products involving non-integer powers of nome. A similar analysis is also carried out at the phase boundary of $H = 0$. Here, the energy gaps scale as N^{-2} which is a characteristic of the PT transition. Also the corresponding partition functions are evaluated and shown to be those of the non-relativistic free fermion system with dispersion relation $\varepsilon \sim k^2$. Using the physical requirement of invariance of the partition function of the lattice model under exchange of rows and columns, i.e. under $\pi/2$ rotation of the lattice, we find interesting mathematical identities between infinite products. We also argue that the $N^{-1/2}$ scaling at the $V = 0$ phase boundary is a feature arising from viewing the standard PT transition of the $H = 0$ phase boundary after $\pi/2$ rotation.

This paper is organized as follows. In section 2, we set notations and review the Bethe ansatz method for bulk properties. Then we discuss classifications of low-lying excitations. In section 3, the formalism for calculating finite-size corrections in energy is developed in line with I and the leading order solution is expressed in terms of level-dependent scaling functions with the scaling variable u. In section 4, the crossover behaviours of the energy gaps for $H > H_c$ and $H < H_c$ are discussed. From this, the class of excitations which remain massless at the facet boundary of $|H| < H_c$ is identified. In section 5, the spectra and the partition functions at $H = H_c$ are derived. We discuss in section 6, the spectra and the partition functions at the antiferromagnetic phase boundary of $H = 0$. From this, we obtain several identities between infinite products. Finally, we summarize and discuss our results in section 7. Some mathematical details are relegated to appendices. Appendix A proves some properties of the scaling function, appendix B contains derivations of the partition function at the $V = 0$ phase boundary, while appendices C and D derive the spectra and the partition function, respectively, at the $H = 0$ phase boundary.

2. Bethe ansatz and energy levels

We consider the asymmetric XXZ chain of N sites whose Hamiltonian is given by

$$\mathcal{H} = (2\sinh\lambda)^{-1}\sum_{i=1}^{N}\left\{\frac{\cosh\lambda}{2}(\sigma_i^z\sigma_{i+1}^z - 1) - \mathrm{e}^{2H}\sigma_i^+\sigma_{i+1}^- - \mathrm{e}^{-2H}\sigma_i^-\sigma_{i+1}^+\right\} - V\sum_{i=1}^{N}\sigma_i^z \qquad (1)$$

where σ_i^a are the Pauli spin operators, $\sigma_{N+1}^a = \sigma_1^a$, and H and V are the horizontal and vertical fields, respectively. The standard interaction parameter Δ has been parametrized as $\Delta = -\cosh\lambda$ with $\lambda > 0$ since we are interested in the region $\Delta < -1$. The front factor is included for later convenience. Below we use the short notation $\alpha \equiv \exp(-2\lambda)$. We also

use the notation for the magnetization as

$$\sum_{i=1}^{N} \sigma_i^z = N - 2Q = 2r \tag{2}$$

where Q is the number of down spins and use $q = Q/N = \frac{1}{2} - \frac{r}{N}$ so that $0 \leqslant q \leqslant 1$ and r takes the integer (half-integer) values for N even (odd). We work in sectors of general but finite r as $N \to \infty$. Since the spectra of (1) for $V = 0$ is symmetric with respect to H and r, we work in the region of $H \geqslant 0$ and $r \geqslant 0$.

The eigenvalues E of $\mathcal{H}$ in the sector r are given by

$$E = -2rV - \sum_{j=1}^{Q} \left(\frac{x_j}{x_j - 1} + \frac{\alpha x_j}{1 - \alpha x_j} \right) \tag{3}$$

where $\{x_j\}$ are the solutions of the Bethe ansatz equation

$$\left(\mathrm{e}^{2H-\lambda} \frac{x_i - 1}{1 - \alpha x_i} \right)^N = (-1)^{Q-1} \prod_{j=1}^{Q} \frac{x_i - \alpha x_j}{x_j - \alpha x_i} \qquad (i = 1, 2, \ldots, Q). \tag{4}$$

(The roots $\{x_j\}$ are related to the standard $\{\alpha_j\}$ notation by $x_j = \exp(\lambda - \mathrm{i}\alpha_j)$.)

The asymmetric XXZ Hamiltonian is the logarithmic derivative of the asymmetric 6-vertex model row-to-row transfer matrix at the extreme anisotropic limit [6]. The eigenvalues Λ of the latter are also expressed in terms of $\{x_j\}$. In this work, we consider the isotropic 6-vertex model, or the F model, in external fields whose six Boltzmann weights are given as $\omega_{1,2} = \exp(\pm(H + V))$, $\omega_{3,4} = \exp(\pm(H - V))$ and $\omega_{5,6} = 2\cosh(\lambda/2)$, respectively. The transfer matrix eigenvalues of the F model are given as

$$-\ln \Lambda = -HN - 2rV - \sum_{j=1}^{Q} \ln \frac{x_j - \exp(-\lambda)}{1 - \exp(-\lambda) x_j} \tag{5}$$

for $H > 0$. The following discussions can be easily extended to the anisotropic 6-vertex model but we consider only the isotropic case for simplicity. We define the phase function or the counting function $Z_N(x)$ by

$$\mathrm{i} Z_N(x) = 2H - \lambda + (1 - q) \ln x + \ln \frac{1 - x^{-1}}{1 - \alpha x} + \frac{1}{N} \sum_{j=1}^{Q} f_Z(x, x_j) \tag{6}$$

with

$$f_Z(x, x') = \ln x' - \ln \frac{1 - \alpha x'/x}{1 - \alpha x/x'} = \ln x' + \sum_{n \neq 0} \frac{\alpha^{|n|}}{n} \left(\frac{x'}{x} \right)^n \tag{7}$$

and the root density function $R_N(x)$ by the derivative of Z_N as

$$\begin{aligned} R_N(x) &= \mathrm{i} x Z_N'(x) \\ &= -q + \frac{x}{x - 1} + \frac{\alpha x}{1 - \alpha x} - \frac{1}{N} \sum_{j=1}^{Q} \left[\sum_{n \neq 0} \alpha^{|n|} \left(\frac{x_j}{x} \right)^n \right] \end{aligned} \tag{8}$$

with $\sum_{n \neq 0}$ denoting the sum over all integers except 0 and $1 < |x| < 1/\alpha$. In terms of Z_N, the Bethe ansatz equation can be rewritten as

$$Z_N(x_j) = \frac{2\pi}{N} I_j \tag{9}$$

where I_j are half-integers (integers) for Q even (odd). The ground state for each Q is obtained if one chooses I_j as

$$\frac{2\pi}{N} I_j = \frac{2\pi}{N}\left(-\frac{Q+1}{2} + j\right) \equiv \phi_j \tag{10}$$

for $j = 1, 2, \ldots, Q$. In the thermodynamic limit, $\{x_j\}$ for the ground state form a continuous curve given by the locus $x = Z_\infty^{-1}(\phi)$ for $-\pi q \leqslant \phi \leqslant \pi q$ where $Z_N^{-1}(\phi)$ denotes the inverse function of $Z_N(x)$.

The simplifying feature for the case of $q = \frac{1}{2}$ and $|H| \leqslant H_c$ is that the root contour becomes closed in the x-plane, as for the case of the stochastic line. Here, H_c is the antiferromagnetic transition point to be given in (14). To find the actual form of $Z_\infty(x)$ for $q = \frac{1}{2}$ and $|H| \leqslant H_c$, one may evaluate the sum in (6) by a contour integration over the circle $|x| = \exp(\lambda - b)$ with $-\lambda < b < \lambda$ using the known expression of $R_\infty(x)$ which is $R_\infty(x) = \sum_n \alpha^n x^n/(1+\alpha^n)$ in our notation. The result is

$$\mathrm{i} Z_\infty(x) = 2H - \lambda + \frac{1}{2}\ln x + \frac{1}{2}\ln|x_0| + \sum_{n\neq 0} \frac{\alpha^n}{n(1+\alpha^n)}(x^n + x_0^n) \tag{11}$$

where $x_0 \equiv \exp(\lambda - b + \pi\mathrm{i})$ is the endpoint of the contour. The conditions $Z_\infty(\exp(\lambda - b \pm \pi\mathrm{i})) = \pm\pi/2$ are met if H is related to x_0 or b by

$$H = \Xi(b) \tag{12}$$

where the real function $\Xi(b)$ defined by [8, 10]

$$\begin{aligned}\Xi(b) &= \frac{b}{2} + \sum_{n=1}^{\infty} \frac{(-1)^n \sinh nb}{n\cosh n\lambda} \\ &= \ln\frac{\cosh(\lambda+b)/2}{\cosh(\lambda-b)/2} - \frac{b}{2} - \sum_{n=1}^{\infty}\frac{(-1)^n\alpha^n \sinh nb}{n\cosh n\lambda}.\end{aligned} \tag{13}$$

The entire antiferromagnetic phase boundary of the lattice model is described by the H-dependent critical vertical field V_c given by [24, 9] $V_c = \Xi(\lambda - b)$ with $-2\lambda < b < 2\lambda$ while that of the asymmetric XXZ chain with normalization as given in (1) is given by (see appendix C) $V_c = \Xi'(b)$. These are shown in figure 1 as a full curve for $\lambda = 2.5$. In both cases, $V_c = 0$ when $b = \pm\lambda$. Thus the critical value H_c of the $V = 0$ phase boundary is given by

$$H_c = \Xi(\lambda). \tag{14}$$

The bulk ground-state energy per site of the chain within the antiferromagnetically ordered region is given as $e_\infty \equiv \lim_{N\to\infty} E/N = -e_0$ where

$$e_0 = \frac{1}{2} + 2\sum_{n=1}^{\infty}\frac{\alpha^n}{1+\alpha^n} \tag{15}$$

and the bulk free energy of the F model is $f_\infty \equiv \lim_{N\to\infty}(-\ln\Lambda)/N = -\lambda/2 - \sum_{n=1}^{\infty} n^{-1}\alpha^{n/2}\tanh n\lambda$.

In the antiferromagnetic phase, finite mass gaps appear in the energy spectra. But these mass gaps are offset by fields and at the antiferromagnetic phase boundary, an infinite number of other levels become degenerate with the ground state in the thermodynamic limit. These degeneracies are lifted for finite but large N. Our aim here is to find these finite-size corrections for arbitrary energy levels. We denote these energy gaps as ΔE and ΔF, respectively: $\Delta E = E - e_\infty N$ and $\Delta F = -\ln\Lambda - f_\infty N$.

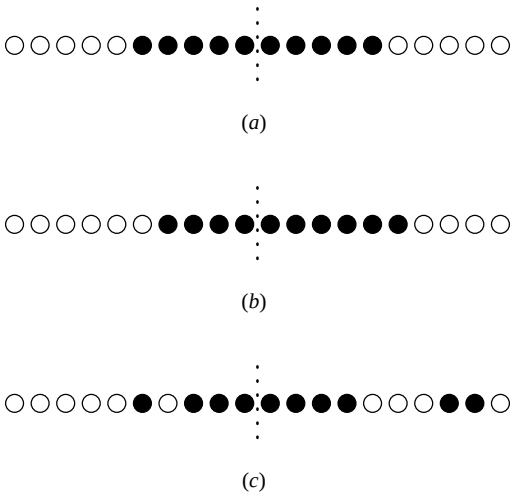

Figure 2. Examples of energy levels for $N = 20$ and $Q = 10$ ($r = 0$). Full circles denote integers included in $\{I_j\}$. (a) The ground state $(0, 0, 0)$. (b) The 1-shifted level $(0, 1, 0)$. (c) An excited level from (b) which has two particle–hole pairs at the right end of the Fermi sea (with positions $p_1 = 2$, $p_2 = 3$, $h_1 = 1$ and $h_2 = 2$) and one particle–hole pair at the left end (with $\bar{p}_1 = 1$ and $\bar{h}_1 = 1$).

The ground state characterized by (10) corresponds to a Fermi sea as depicted in figure 2(a) for r=0. Other energy levels are obtained if other sets of $\{I_j\}$ are chosen. An important class of levels is the m-shifted levels where $\{I_j\}$ are shifted by an integer m from that of the ground state, i.e. $2\pi I_j/N = \phi_{j+m}$. These states are denoted as $(r, m, 0)$. figure 2(b) shows the 1-shifted level $(0, 1, 0)$. Further excitations are obtained by creating from the m-shifted states an equal numbers of particles and holes near the two ends of the Fermi sea. Excited levels are then characterized by their particle and hole positions. The particle (hole) positions near the right-hand side of the Fermi sea can be specified by a set of integers $\{p_k\}, (\{h_k\})$ which are related to the index j in ϕ_j as $j = Q + m + p_k(Q + m + 1 - h_k)$, for $k = 1, 2, \ldots, n_+$, n_+ being the number of particle-hole pairs, and $1 \leqslant p_1 < p_2 < \cdots < p_{n_+}$ ($1 \leqslant h_1 < h_2 < \cdots < h_{n_+}$). Particles (holes) near the left-hand side may be labelled similarly by $\{\bar{p}_k\}(\{\bar{h}_k\})$ with $j = 1 + m - \bar{p}_k(m + \bar{h}_k)$, for $k = 1, 2, \ldots, n_-$ and $1 \leqslant \bar{p}_1 < \bar{p}_2 < \cdots < \bar{p}_{n_-}(1 \leqslant \bar{h}_1 < \bar{h}_2 < \cdots < \bar{h}_{n_-})$. Such excitation configurations are denoted collectively by $\mathcal{P}$. General levels are then labelled as $(r, m, \mathcal{P})$. Figure 2(c) shows an example of particle–hole excitations. In [3], it was shown for the critical region that levels obtained in this way account for all the low-lying excitations which are expected to appear from the central charge $c = 1$ conformal field theory. Here, we also assume that all the low-lying excitations are generated in this manner.

When the particle–hole configurations differ from the ground state only at finite distances away from the two ends of the Fermi sea, finite-size corrections in energies are determined by the analytic property of $Z_\infty(x)$ near $x = x_0$. However, the root density vanishes at $x = x_c^0 \equiv \mathrm{e}^{\pi \mathrm{i}}$ which is the endpoint of the root contour for $H = H_c$. Therefore $Z_\infty^{-1}(\phi)$ exhibits a square-root singularity at $\phi = \pm\pi/2$. The same phenomenon was the origin of the unusual $N^{-3/2}$ scaling of the energy gaps along the stochastic line and one can expect that a similar mechanism produces $N^{-1/2}$ scaling in the present case. On the other hand, for $|H| < H_c$, $\mathrm{O}(N^{-1})$ variations in ϕ near $\phi = \pm\pi/2$ cause, via $Z_\infty^{-1}(\phi)$, $\mathrm{O}(N^{-1})$ variations in the x-plane and hence the finite-size corrections take the form of power series in N^{-1}.

What is special at the antiferromagnetic phase boundary is that the real parts of the energy gaps scale as N^{-2} which is the characteristic of the PT transition. These features are born out explicitly below.

3. Energy gaps for H near H_c

In this section, we derive the leading-order finite-size correction of the energy gaps ΔE and ΔF for general levels with $(H - H_c)N$ as a scaling variable. To find the energy gaps for H near H_c, we employ the method of I. Thus, for finite but large N and for levels whose energies are close to that of the ground state, we assume, following I, that there exists in the complex x-plane a point x_c near $x_c^0 = \mathrm{e}^{\pi \mathrm{i}}$ such that $Z_N'(x_c) = 0$, $Z_N(x)$ itself having a branch cut passing through x_c, and that near x_c, $Z_N(x)$ has the expansion of the form

$$\mathrm{i}Z_N(x) = \pm \mathrm{i}\pi q + y_\pm \frac{\pi}{N} + \frac{1}{a_1^2}(x - x_c)^2 + \mathrm{O}((x - x_c)^3) \tag{16}$$

where the upper (lower) sign refers to the assumed value of $\mathrm{i}Z_N(x)$ at $x = x_c$ ($x = x_c \mathrm{e}^{-2\pi \mathrm{i}}$). This amounts to assuming

$$Z_N^{-1}\left(\pm \pi q + \frac{\pi}{N}\xi\right) = x_c^\pm \pm \mathrm{i}a_1 \sqrt{y_\pm - \mathrm{i}\xi}\sqrt{\frac{\pi}{N}} + \mathrm{O}(N^{-1}) \tag{17}$$

for $\xi \sim \mathrm{O}(1)$ with $x_c^+ = x_c$ and $x_c^- = x_c \mathrm{e}^{-2\pi \mathrm{i}}$.

The constants x_c, a_1, $y_\pm$, etc are all level dependent and should be determined self-consistently. But, first we assume they are known and evaluate the finite sums of the form

$$S[f] = \sum_{j=1}^{Q} f(x_j) = \sum_{j=1}^{Q} f\left(Z_N^{-1}\left(\frac{2\pi}{N} I_j\right)\right) \tag{18}$$

to $\mathrm{O}(1/\sqrt{N})$ for arbitrary $f(x')$. Following the same steps as in I, but generalizing to levels with $m \neq 0$, we find

$$\begin{aligned} S[f] = \frac{N}{2\pi \mathrm{i}} \oint f(x) R_N(x) \frac{\mathrm{d}x}{x} + \left(m + \frac{\mathrm{i}}{2} y_+\right) f(x_c) - \left(m + \frac{\mathrm{i}}{2} y_-\right) f(x_c \mathrm{e}^{-2\pi \mathrm{i}}) \\ + a_1 f'(x_c) Y_1(y_+, y_-) \sqrt{\frac{\pi}{N}} + \mathrm{O}(N^{-1}) \end{aligned} \tag{19}$$

where the integral is over a closed contour in the annulus $1 < |x| < 1/\alpha$ and $Y_1(y_+, y_-)$ is defined below. To define Y_1, we first introduce two functions $J_+(y)$ and $J_-(y)$ of complex variable defined for $\Im y > 0$ and $\Im y < 0$, respectively, as

$$J_\pm(y) = \frac{1}{2} \int_0^\infty \frac{\sqrt{y + t} - \sqrt{y - t}}{\mathrm{e}^{\pi t} - 1} \, \mathrm{d}t \pm \frac{\mathrm{i}}{2} y^{1/2} - \frac{1}{3} y^{3/2} \tag{20}$$

with the branch cut of the square roots at the negative real axis. As shown in appendix A, $J_\pm(y)$ satisfy the recursion relations

$$J_\pm(y \pm 2\mathrm{i}) = J_\pm(y) \mp \mathrm{i}\sqrt{y}. \tag{21}$$

Thus, we may extend the definition of $J_+(y)$ ($J_-(y)$) into the half plane $\Im y \leqslant 0$ ($\Im y \geqslant 0$) using relation (21) recursively. Having defined $J_\pm(y)$, we then give the expression of Y_1

for the general level $(r, m, \mathcal{P})$:

$$Y_1(y_+, y_-) = J_+(y_+ + \mathrm{i} - 2\mathrm{i}m) + J_-(y_- - \mathrm{i} - 2\mathrm{i}m) + \mathrm{i}\sum_{k=1}^{n_+}\left(\sqrt{y_+ + \mathrm{i}(1-2m-2p_k)} - \sqrt{y_+ - \mathrm{i}(1+2m-2h_k)}\right) - \mathrm{i}\sum_{k=1}^{n_-}\left(\sqrt{y_- - \mathrm{i}(1+2m-2\bar{p}_k)} - \sqrt{y_- + \mathrm{i}(1-2m-2\bar{h}_k)}\right). \tag{22}$$

The first two terms in (22) are contributions for the m-shifted levels and the sums in the second (third) line account for particle–hole pairs created at the right (left) end of the Fermi sea. When $m = 0$ and $y_+ = y_-$, $Y_1(y, y)$ reduces to $-Y_1(y)$ defined in I.

Applying (19) to (8), we then obtain the solution for R_N as

$$R_N(x) = R_\infty(x) + \frac{r}{N} + \frac{1}{N}\sum_{n\neq 0}\frac{\alpha^{|n|}}{1+\alpha^{|n|}}\left(\frac{x}{x_c}\right)^n \times\left(\frac{y_+ - y_-}{2\mathrm{i}} + \frac{n}{x_c}a_1 Y_1(y_+, y_-)\sqrt{\frac{\pi}{N}}\right) + \mathrm{O}(N^{-2}). \tag{23}$$

Having obtained $R_N(x)$ to $\mathrm{O}(N^{-3/2})$, we can evaluate $S[f]$ to $\mathrm{O}(N^{-1/2})$ for any $f(x')$. In particular, applying the general sum formula to $f(x') = f_Z(x, x')$ given in (7), $Z_N(x)$ can be evaluated to $\mathrm{O}(N^{-3/2})$. Evaluating the latter and its two derivatives at $x = x_c^{\pm}$, one obtains four self-consistency equations for $y_\pm$, x_c and a_1 from (16). Solving them perturbatively, we find

$$y_\pm = (\pm 2r + m)\mathrm{i} + u + \mathrm{O}(N^{-1/2}) \tag{24}$$

$$x_c = \mathrm{e}^{\pi\mathrm{i}} + \frac{2re_0}{e_1^2}\frac{1}{N} + \mathrm{O}(N^{-2}) \tag{25}$$

$$a_1 = \frac{\sqrt{2}}{e_1} + \mathrm{O}(N^{-1}) \tag{26}$$

where e_0 is given in (15), e_1 is a positive real constant defined as

$$e_1 \equiv (-R'_\infty(-1))^{1/2} = (-\Xi''(\lambda))^{1/2} = \left(\frac{1}{4} + 2\sum_{n=1}^{\infty} n(-1)^n\frac{\alpha^n}{1+\alpha^n}\right)^{1/2} \tag{27}$$

and u is the scaling variable

$$u = (H - H_c)N/\pi \tag{28}$$

which is assumed fixed as $N \to \infty$. Having determined $y_\pm$, x_c and a_1 to necessary orders, we are now in a position to evaluate ΔE and ΔF. Applying (19) together with (23) to (3) and using the perturbative solutions, we find

$$\Delta E \equiv E - e_\infty N = -2rV + e_1\mathcal{Y}_1^{(r,m,\mathcal{P})}\sqrt{\frac{2\pi}{N}} + \mathrm{O}(N^{-1}) \tag{29}$$

where $e_\infty = -e_0$ and $\mathcal{Y}_1^{(r,m,\mathcal{P})}$ is the value of $Y_1(y_+, y_-)$ at $y_\pm = u + (\pm 2r + m)\mathrm{i}$:

$$\mathcal{Y}_1^{(r,m,\mathcal{P})} = J_+(u + \mathrm{i}(2r - m + 1)) + J_-(u - \mathrm{i}(2r + m + 1)) + \mathrm{i}\sum_{k=1}^{n_+}\left(\sqrt{u + \mathrm{i}(2r - m + 1 - 2p_k)} - \sqrt{u + \mathrm{i}(2r - m - 1 + 2h_k)}\right) - \mathrm{i}\sum_{k=1}^{n_-}\left(\sqrt{u - \mathrm{i}(2r + m + 1 - 2\bar{p}_k)} - \sqrt{u - \mathrm{i}(2r + m - 1 + 2\bar{h}_k)}\right). \tag{30}$$

Here, $J_{\pm}(y)$ and u are given in (20) and (28), respectively. $\mathcal{Y}_1^{(r,m,\mathcal{P})}$, regarded as a function of the scaling variable u, is then the scaling function. A similar calculation for the F model leads to

$$\Delta F \equiv -\ln\Lambda - f_\infty N = -\mathrm{i}\pi m - 2rV + \frac{e_2}{e_1}\mathcal{Y}_1^{(r,m,\mathcal{P})}\sqrt{\frac{2\pi}{N}} + \mathrm{O}(N^{-1}) \tag{31}$$

where the constant e_2 is given as

$$e_2 \equiv \Xi'(0) = \frac{1}{2} + \sum_{n=1}^{\infty}\frac{(-1)^n}{\cosh n\lambda}. \tag{32}$$

Note that ΔF has an imaginary term due to Λ being negative for m odd. Apart from this, all energy gaps at $V = 0$ scale as $N^{-1/2}$ and all the level dependences are encoded in the scaling function $\mathcal{Y}_1^{(r,m,\mathcal{P})}$. Higher-order corrections which come as a power series in $N^{-1/2}$ can be calculated perturbatively using the method similar to that of I.

4. Crossover behaviours for $H \neq H_c$

Equations (29) and (31) are obtained with the scaling variable u fixed. By considering the limits $u \to \pm\infty$, we can derive how the spectra crossover to those of the critical and massive phases. First consider the case $H > H_c$ where $u \to \infty$ as $N \to \infty$. From (20), one can show that, as $u \to \infty$,

$$J_{\pm}(u \pm \mathrm{i}a) = -\frac{1}{3}u^{3/2} \mp \frac{\mathrm{i}}{2}(a-1)u^{1/2} + \left(\frac{a^2}{8} - \frac{a}{4} + \frac{1}{12}\right)u^{-1/2} + \mathrm{O}(u^{-3/2}). \tag{33}$$

Using this in (30), $\mathcal{Y}_1^{(r,m,\mathcal{P})}$ becomes

$$\mathcal{Y}_1^{(r,m,\mathcal{P})} = -\frac{2}{3}u^{3/2} + \mathrm{i}mu^{1/2} + \left(\frac{m^2}{4} + r^2 - \frac{1}{12} + \mathcal{N} + \overline{\mathcal{N}}\right)u^{-1/2} + \mathrm{O}(u^{-3/2}) \tag{34}$$

with $\mathcal{N} = \sum_{k=1}^{n_+}(p_k + h_k - 1)$ and $\overline{\mathcal{N}} = \sum_{k=1}^{n_-}(\bar{p}_k + \bar{h}_k - 1)$. The first term in (34) contributes a bulk energy term proportional to $(H - H_c)^{3/2}N$ to ΔE and ΔF, the second an O(1) imaginary term and the third a real one proportional to $(H - H_c)^{-1/2}N^{-1}$. These are exactly those which appear in the critical phase as shown in [3] and show the complete operator content of the Gaussian model. In the Coulomb gas picture, m and r are the spin wave and vortex quantum numbers, respectively, characterizing primary operators of the $c = 1$ conformal field theory whose Gaussian coupling constant g is 2, and $\mathcal{N}$ and $\overline{\mathcal{N}}$ account for the conformal towers generated from the primary operators. Higher-order corrections in (29) and (31) not discussed here would give terms which are higher orders in $(H - H_c)$.

Next consider the case $H < H_c$. Now $u \to -\infty$ as $N \to \infty$ and one has to be careful about the branch cut of the square root. We find

$$J_{\pm}(u \pm \mathrm{i}a) = \pm\frac{\mathrm{i}}{3}|u|^{3/2} + G_{\pm}|u|^{1/2} + \mathrm{O}(|u|^{-1/2}) \tag{35}$$

with $G_{\pm} = |a-1|/2$ for $a > 0$ or for a negative odd integers but, for $a \leqslant 0$ and even integers, $G_+ = (|a|-1)/2$ while $G_- = (|a|+3)/2$. Using this, we find the leading order of $\mathcal{Y}_1^{(r,m,\mathcal{P})}$ for levels $(r, m, 0)$ as $\mathcal{Y}_1^{(r,m,0)} = \max(2r, |m|)|u|^{1/2}$ if $(2r + m)$ is even and $\mathcal{Y}_1^{(r,m,0)} = \max(2r, |m-1|)|u|^{1/2}$ if $(2r + m)$ is odd. Thus, when m is in the range $-(2r+1) < m \leqslant (2r+1)$, $\mathcal{Y}_1^{(r,m,0)} = 2r|u|^{1/2} + \mathrm{O}(|u|^{-1/2})$. In view of the contributions from particle–hole excitations in (30), we note that, for $-(2r+1) < m \leqslant (2r+1)$, particles

at positions satisfying the condition $2r-m+1-2p_k \geqslant 0$ or $2r+m+1-2\bar{p}_k > 0$ contribute $-|u|^{1/2}$ but those violating the condition and each hole contribute $|u|^{1/2}$. Thus, when all particle positions satisfy the condition, or equivalently, when the last positions satisfy the condition

$$-(2r+1) < m \leqslant (2r+1) \qquad 2p_{n_+} \leqslant 2r-m+1 \qquad 2\bar{p}_{n_-} < 2r+m+1 \tag{36}$$

then all particle contributions are cancelled by holes. Thus, for such levels, $\mathcal{Y}_1^{(r,m,\mathcal{P})} = 2r|u|^{1/2} + \mathrm{O}(|u|^{-1/2})$ and ΔE becomes

$$\Delta E = -2rV + 2\sqrt{2}e_1(H_c - H)^{1/2}r \tag{37}$$

as $H \to H_c$ in the thermodynamic limit. The second term in (37) is the mass gap of the antiferromagnetic phase of the asymmetric XXZ chain whose general expression is given in (C.11) and also in [1]. A corresponding expression for the lattice model is

$$\Delta F = -\mathrm{i}\pi m - 2rV + 2\sqrt{2}e_2e_1^{-1}(H_c - H)^{1/2}r. \tag{38}$$

For levels which do not satisfy (36), the mass gap becomes higher by O(1). Equations (37) and (38) are derived for $r \geqslant 0$; for general r, the factor r in their last terms should be replaced by $|r|$ due to the spin reversal symmetry. When $2rV$ is equal to the mass gap, all levels $(r, m, \mathcal{P})$ satisfying (36) become degenerate with the ground-state energy in the thermodynamic limit. For $V > 0$, this level crossing happens only for $r > 0$. Finite-size corrections of these degenerate energies will be discussed in section 6.

A special mention is needed for $r = 0$ which is the half-filled sector for N even. Here, only two levels $(0, 0, 0)$ and $(0, 1, 0)$ satisfy (36). The latter which has momentum π is the exponentially degenerate second-largest eigenvalue of the transfer matrix as discussed in [25]. Such an exponential degeneracy is reflected in the large u behaviour of $\mathcal{Y}_1^{(r,m,\mathcal{P})}$. When expanded as a power series in $|u|^{-1}$, both $\mathcal{Y}_1^{(0,0,0)}$ and $\mathcal{Y}_1^{(0,1,0)}$ have vanishing coefficients to all orders in the series.

5. Spectra and partition functions at $H = H_c$ and $V = 0$

Now we consider the case $H = H_c$ with $V = 0$ (the points A in figure 1). Since $u = 0$ in this case, one needs to evaluate $J_\pm(\mathrm{i}a)$ for integer values of a. Successive application of the recursion relation (21) yields,

$$J_+(\mathrm{i}a) = \begin{cases} \sqrt{-\mathrm{i}} \displaystyle\sum_{j=0}^{(a-3)/2} \sqrt{1+2j} - \sqrt{-\mathrm{i}}c_1 & \text{if } a > 0 \text{ and odd} \\ \sqrt{\mathrm{i}} \displaystyle\sum_{j=0}^{(|a|-1)/2} \sqrt{1+2j} - \sqrt{-\mathrm{i}}c_1 & \text{if } a < 0 \text{ and odd} \\ \sqrt{-\mathrm{i}} \displaystyle\sum_{j=0}^{(a-2)/2} \sqrt{2j} + \sqrt{-\mathrm{i}}c_2 & \text{if } a > 0 \text{ and even} \\ \sqrt{\mathrm{i}} \displaystyle\sum_{j=0}^{|a|/2} \sqrt{2j} + \sqrt{-\mathrm{i}}c_2 & \text{if } a \leqslant 0 \text{ and even} \end{cases} \tag{39}$$

and $J_-(-\mathrm{i}a) = J_+(\mathrm{i}a)^*$ where the positive numbers c_1 and c_2, called anomaly, are given as

$$c_1 \equiv -J_+(\mathrm{i})/\sqrt{-\mathrm{i}} = \frac{1}{6} - \frac{1}{2\mathrm{i}} \int_0^\infty \frac{\sqrt{1+\mathrm{i}t} - \sqrt{1-\mathrm{i}t}}{\mathrm{e}^{\pi t} - 1}\, \mathrm{d}t \tag{40}$$

$$c_2 \equiv J_+(0)/\sqrt{-\mathrm{i}} = \zeta\left(\tfrac{3}{2}\right) / \left(2\sqrt{2}\pi\right) = 0.293\,995\,52 \tag{41}$$

with $\zeta(z)$ the Riemann zeta function. We will see later in an indirect way that $c_1 = (\sqrt{2}-1)\zeta(\frac{3}{2})/(4\pi) = 0.086\,109\,29$ (equation (66)).

Using (39) in (30) with $u = 0$, one can read off $\mathcal{Y}_1^{(r,m,\mathcal{P})}$ for arbitrary levels. It is a sum of square-root of integers and the anomaly term. We give a few examples:

(i) m-shifted levels with $-(2r+1) < m \leqslant (2r+1)$:

$$\mathcal{Y}_1^{(r,m,0)} = -\sqrt{2}c_1 + \sqrt{-\mathrm{i}}\sum_{j=0}^{r-m/2-1}\sqrt{1+2j} + \sqrt{\mathrm{i}}\sum_{j=0}^{r+m/2-1}\sqrt{1+2j} \tag{42}$$

for $(2r+m)$ even and

$$\mathcal{Y}_1^{(r,m,0)} = \sqrt{2}c_2 + \sqrt{-\mathrm{i}}\sum_{j=0}^{r-(m+1)/2}\sqrt{2j} + \sqrt{\mathrm{i}}\sum_{j=0}^{r+(m-1)/2}\sqrt{2j} \tag{43}$$

for $(2r+m)$ odd.

(ii) m-shifted levels in sector $r = 0$:

$$\mathcal{Y}_1^{(0,m,0)} = \begin{cases} 2\sqrt{\mathrm{i}}\displaystyle\sum_{j=0}^{m/2-1}\sqrt{1+2j} - \sqrt{2}c_1 & \text{for } m > 0 \text{ even} \\ 2\sqrt{\mathrm{i}}\displaystyle\sum_{j=0}^{(m-1)/2}\sqrt{2j} + \sqrt{2}c_2 & \text{for } m > 0 \text{ odd.} \end{cases} \tag{44}$$

For $m < 0$, $\mathcal{Y}_1^{(0,m,0)}$ is the complex conjugate of $\mathcal{Y}_1^{(0,|m|,0)}$.

(iii) One particle–hole pair excitation from $(0,0,0)$:

$$\mathcal{Y}_1^{(0,0,\mathcal{P})} = -\sqrt{2}c_1 + \sqrt{\mathrm{i}}\sqrt{2p_1-1} + \sqrt{-\mathrm{i}}\sqrt{2h_1-1} \tag{45}$$

with the positive integers p_1 (h_1) being the position of the particle (hole).

We have compared the above predictions with existing numerical data of ΔE obtained by solving the Bethe ansatz equation for finite N [26, 2]. Extrapolations of available data ($N \leqslant 80$ for levels $(0,0,0)$ and $(1,0,0)$, $N \leqslant 68$ for $(0,2,0)$, $N \leqslant 56$ for $(2,0,0)$) all show excellent convergence to the expected exact values with 4–6 digit accuracies.

Having obtained the leading finite-size corrections for arbitrary levels, one can go further to evaluate the partition functions in the scaling limit. We consider the partition function of the asymmetric XXZ chain at temperature T (in units of the Boltzmann constant) and the lattice model on a $N \times M$ lattice with periodic boundary conditions defined by $\mathcal{Z}_E = \sum \exp(-\Delta E/T)$ and $\mathcal{Z}_F = \sum \exp(-M\Delta F)$, respectively, where the sums are over all states and the bulk part $\exp(-Ne_\infty/T)$ for the chain and $\exp(-MNf_\infty)$ for the lattice model has been taken out. To obtain a non-trivial limit, we take the thermodynamic limit with $\sqrt{N}T$ or $MN^{-1/2}$ fixed. In this scaling limit, the $\mathrm{O}(N^{-1/2})$ part of the energy gaps produces finite contributions while those levels which are not degenerate with the ground state in the thermodynamic limit need not be considered.

Considering $\mathcal{Z}_F$ first, we can write from (31),

$$\mathcal{Z}_F = \sum_{(r,m,\mathcal{P})} (-1)^{mM} \exp\left(-\frac{e_2 M}{e_1}\sqrt{\frac{2\pi}{N}}\mathcal{Y}_1^{(r,m,\mathcal{P})}\right). \tag{46}$$

The sum is conveniently expressed in terms of a complex parameter $\boldsymbol{q}$ which we call nome:

$$\boldsymbol{q} = \exp\left(-\pi\sqrt{\mathrm{i}\tau}\right) \tag{47}$$

where

$$\tau = 2e_2^2 M^2/(\pi e_1^2 N). \tag{48}$$

Derivation of the partition function is relegated to appendix B. Our final result for $\mathcal{Z}_F$ is

$$\mathcal{Z}_F = \begin{cases} \mathcal{Z}_1(\boldsymbol{q}) \pm \mathcal{Z}_2(\boldsymbol{q}) + \mathcal{Z}_3(\boldsymbol{q}) & \text{for } M \text{ even} \\ \pm\mathcal{Z}_1(\boldsymbol{q}) + \mathcal{Z}_2(\boldsymbol{q}) \mp \mathcal{Z}_3(\boldsymbol{q}) & \text{for } M \text{ odd} \end{cases} \tag{49}$$

where the upper (lower) sign is for N even (odd) and $\mathcal{Z}_i(\boldsymbol{q})$ are defined as

$$\mathcal{Z}_1(\boldsymbol{q}) = \tfrac{1}{2}(\boldsymbol{q}\bar{\boldsymbol{q}})^{-c_1} \prod_{j=-\infty}^{\infty} \left(1 + \boldsymbol{q}^{\sqrt{1+2j}}\right)\left(1 + \bar{\boldsymbol{q}}^{\sqrt{1+2j}}\right) \tag{50}$$

$$\mathcal{Z}_2(\boldsymbol{q}) = \tfrac{1}{2}(\boldsymbol{q}\bar{\boldsymbol{q}})^{-c_1} \prod_{j=-\infty}^{\infty} \left(1 - \boldsymbol{q}^{\sqrt{1+2j}}\right)\left(1 - \bar{\boldsymbol{q}}^{\sqrt{1+2j}}\right) \tag{51}$$

$$\mathcal{Z}_3(\boldsymbol{q}) = \tfrac{1}{2}(\boldsymbol{q}\bar{\boldsymbol{q}})^{c_2} \prod_{j=-\infty}^{\infty} \left(1 + \boldsymbol{q}^{\sqrt{2j}}\right)\left(1 + \bar{\boldsymbol{q}}^{\sqrt{2j}}\right) \tag{52}$$

with c_1 and c_2 given in (40) and (41), respectively, and $\bar{\boldsymbol{q}}$ denoting the complex conjugate of $\boldsymbol{q}$.

For the asymmetric XXZ chain, we have

$$\mathcal{Z}_E = \sum_{(r,m,\mathcal{P})} \exp\left(-\frac{e_1}{T}\sqrt{\frac{2\pi}{N}}\mathcal{Y}_1^{(r,m,\mathcal{P})}\right). \tag{53}$$

In this case, we can simply use the result of $\mathcal{Z}_F$ for M even by redefining the nome as $\boldsymbol{q}' = \exp(-e_1\sqrt{2\pi \mathrm{i}/N}/T)$. Using this, we then have

$$\mathcal{Z}_E = \mathcal{Z}_1(\boldsymbol{q}') \pm \mathcal{Z}_2(\boldsymbol{q}') + \mathcal{Z}_3(\boldsymbol{q}') \tag{54}$$

where the $+$ $(-)$ sign is for N even (odd).

6. Spectra and partition functions at $H = 0$ and $V = V_c$

The partition function of the isotropic lattice model on a $N \times M$ lattice should be invariant under rotation of the lattice by 90°. After the rotation, roles of H and V are also interchanged. Thus, we expect an invariance of the partition functions under $N \leftrightarrow M$ and $H \leftrightarrow V$. When the system is in the critical phase, this symmetry is manifest by the modular covariance of the partition function. Modular invariance plays an important role in classifying the conformal invariant theories and in revealing their mathematical structures. The present system is in a way a non-relativistic limit of the CFT and it is of interest to find the analogue of the modular transformation. For this purpose, we have also calculated the energy spectra of the two models at $|H| \leqslant H_c$ for those which are low-lying near $V = V_c$ where V_c is the H-dependent critical vertical field. The method employed is similar to the case of $H = H_c$ except that the ansatz for $Z_N^{-1}(\phi)$ takes a different form and that only those levels satisfying the condition given in equation (36) and $r \geqslant 0$ come into the working. More details are given in appendix C. To compare the result with that of the $V = 0$ phase boundary (the points A in figure 1), we consider only the $H = 0$ phase boundary (the points B in figure 1). The result for the F model at $H = 0$ is

$$\Delta F = -\pi \mathrm{i} m + 2r(H_c - V) + \frac{e_1^2}{2e_2^2}\mathcal{Y}_4^{(r,m,\mathcal{P})}(\pi/N)^2 + \mathrm{O}(N^{-3}) \tag{55}$$

where H_c, e_1 and e_2 are given in (14), (27) and (32), respectively, and $\mathcal{Y}_4^{(r,m,\mathcal{P})}$ is given by

$$\mathcal{Y}_4^{(r,m,\mathcal{P})} = \frac{8}{3}r^3 - \frac{2}{3}r + 2rm^2 - \sum_{k=1}^{n_+}[(2r - m + 1 - 2p_k)^2 - (2r - m - 1 + 2h_k)^2] - \sum_{k=1}^{n_-}[(2r + m + 1 - 2\bar{p}_k)^2 - (2r + m - 1 + 2\bar{h}_k)^2] \tag{56}$$

while that for the chain at $H = 0$ is

$$\Delta E = 2r(e_2 - V) + \frac{e_4}{2e_2^2}\mathcal{Y}_4^{(r,m,\mathcal{P})}(\pi/N)^2 + \mathrm{O}(N^{-3}) \tag{57}$$

where $e_4 \equiv -\Xi'''(0) = \sum_{n=1}^{\infty}(-1)^{n+1}n^2/\cosh n\lambda$. Note that V_c at $H = 0$ is the same as H_c for the lattice due to isotropy, but it is $e_2 = \Xi'(0)$ for the chain. For H not equal to zero, imaginary $\mathrm{O}(N^{-1})$ terms appear in ΔE and ΔF. However, the real parts are $\mathrm{O}(N^{-2})$ for all $|H| < H_c$.

From the result of the energy gaps, we are able to calculate the partition functions as in the previous section. We consider the lattice case first since it is more general. To compare it with (49), we interchange M and N in (55) and offset the mass gap by setting $V = H_c$. Then the partition function of an $M \times N$ lattice at the $H = 0$ phase boundary is

$$\mathcal{Z}_F = \sum_{(r,m,\mathcal{P})}(-1)^{mN}\exp\left(-\frac{\pi}{\tau}\mathcal{Y}_4^{(r,m,\mathcal{P})}\right) \tag{58}$$

with $\tau = 2e_2^2M^2/(\pi e_1^2N)$ as was given previously in (48). $\mathcal{Z}_F$ evaluated in this way should be the same as that obtained in section 5 by symmetry. To express the partition function in a compact way, we define the new nome as

$$\boldsymbol{p} = \exp(-\pi/\tau). \tag{59}$$

This is analogous to the nome corresponding to the conjugate modulus in elliptic functions [7]. After performing the sums over the levels, we find $\mathcal{Z}_F$ as

$$\mathcal{Z}_F = \begin{cases} \tilde{\mathcal{Z}}_1(\boldsymbol{p}) \pm \tilde{\mathcal{Z}}_2(\boldsymbol{p}) + \tilde{\mathcal{Z}}_3(\boldsymbol{p}) & \text{for } M \text{ even} \\ \pm\tilde{\mathcal{Z}}_1(\boldsymbol{p}) + \tilde{\mathcal{Z}}_2(\boldsymbol{p}) \mp \tilde{\mathcal{Z}}_3(\boldsymbol{p}) & \text{for } M \text{ odd} \end{cases} \tag{60}$$

where the upper (lower) sign is for N even (odd) and $\tilde{\mathcal{Z}}_i$ are defined as

$$\tilde{\mathcal{Z}}_1(\boldsymbol{p}) = \tfrac{1}{2}\prod_{j=-\infty}^{\infty}(1 + \boldsymbol{p}^{(1+2j)^2}) \tag{61}$$

$$\tilde{\mathcal{Z}}_2(\boldsymbol{p}) = \tfrac{1}{2}\prod_{j=-\infty}^{\infty}(1 + \boldsymbol{p}^{4j^2}) \tag{62}$$

$$\tilde{\mathcal{Z}}_3(\boldsymbol{p}) = \tfrac{1}{2}\prod_{j=-\infty}^{\infty}(1 - \boldsymbol{p}^{(1+2j)^2}). \tag{63}$$

Derivation of (60) is sketched in appendix D. The corresponding partition function $\tilde{\mathcal{Z}}_E$ for the asymmetric XXZ chain with M sites at temperature T can be obtained from the N even result of (60) with $\boldsymbol{p}$ replaced by $\boldsymbol{p}' = \exp(-e_4\pi^2/(2e_2^2M^2T))$;

$$\tilde{\mathcal{Z}}_E = \tilde{\mathcal{Z}}_1(\boldsymbol{p}') \pm \tilde{\mathcal{Z}}_3(\boldsymbol{p}') + \tilde{\mathcal{Z}}_2(\boldsymbol{p}') \tag{64}$$

with the $+$ $(-)$ sign for M even (odd).

Equating (49) and (60) for the four cases of parity of M and N, we find

$$\mathcal{Z}_i(\boldsymbol{q}) = \tilde{\mathcal{Z}}_i(\boldsymbol{p}) \tag{65}$$

for all $i = 1, 2, 3$, and for any τ where $\boldsymbol{q}$ and $\boldsymbol{p}$ are related to τ by (47) and (59), respectively. This is an analogue of the conjugate modulus transformation of the elliptic functions. These identities are obtained by calculating the physically same quantity in two independent ways and are confirmed numerically. However, we are not able to prove them directly. A byproduct of the identities is the analytic expression of c_1 mentioned below equation (41). Taking the $\tau \to \infty$ limit in $\ln \tilde{\mathcal{Z}}_1(\exp(-\pi/\tau))$, and evaluating the leading-order contributions using (A.3), one easily obtains $\ln \tilde{\mathcal{Z}}_1(\exp(-\pi/\tau)) \longrightarrow \frac{1}{2}(\sqrt{2}-1)\zeta(\frac{3}{2})\sqrt{\tau/2}$. Comparing this with $\mathcal{Z}_1(\exp(-\pi\sqrt{\mathrm{i}\tau}))$, one obtains the alternate result for c_1 as

$$c_1 = (\sqrt{2}-1)\zeta(\tfrac{3}{2})/(4\pi). \tag{66}$$

Similar steps using $\tilde{\mathcal{Z}}_3(\exp(-\pi/\tau))$ confirm the leading-order behaviour of $\mathcal{Z}_3(\boldsymbol{q})$ for small $\boldsymbol{q}$.

7. Discussion

In this paper, we have presented Bethe ansatz solutions for the finite-size corrections of the energy gaps at the antiferromagnetic phase transition for both the asymmetric XXZ chain and the isotropic 6-vertex model or the F model. Furthermore, all the low-lying levels are summed to obtain explicit expressions for partition functions. As a byproduct, interesting identities between several infinite products were found. Main results of this paper are (29) and (31) for energy gaps at the $V = 0$ phase boundary, (57) and (55) for the same at the $H = 0$ phase boundary, (49) and (60) for the partition functions and the three identities (65).

The finite-size corrections of the energy gaps are calculated using the method developed in I [6]. Here, the phase function appearing in the Bethe ansatz solution is assumed to take a certain form and is determined self-consistently. At $H = H_c$ and $V = 0$, the finite-size corrections take the form of power series in $N^{-1/2}$ because of the fact that the density of roots for the ground state vanishes at the endpoints of the root contour. The same is true on the stochastic line treated in I but, in the latter case, the leading $\mathrm{O}(N^{-1/2})$ term is absent resulting in the $N^{-3/2}$ scaling of energy gaps. For $|H| < H_c$ and $V = V_c$, the finite-size corrections come out as a power series in N^{-1}. The leading $\mathrm{O}(N^{-1})$ term is imaginary and the real contribution appears from $\mathrm{O}(N^{-2})$. This N^{-2} scaling is the characteristic of the PT transition and is more generic. The points $H = \pm H_c$ and $V = 0$ of the phase boundary are special in that the direction of the 'time' of the Hamiltonian (1) and the row-to-row transfer matrix of the lattice model is orthogonal to the direction of the field and tangential to the phase boundary in the H–V plane.

The partition function at $H = 0$ and $V = V_c$ given in (60) is actually that of one-dimensional non-relativistic free fermions with dispersion relation $\varepsilon = Ak^2$, A being a constant. To make exact correspondence with (60), we simply require that the momenta k be an even or odd integer multiple of π/L, L being the length of the system, depending on the parity of the total number of fermions. Thus, the effective theory on the $H = 0$ antiferromagnetic phase boundary is that of non-relativistic free fermions with the inverse temperature or the number of rows playing the role of imaginary time. This is also true at $q = 0$ or $q = 1$ (the broken curves in figure 1) where the transition can be viewed as the PT-type commensurate–incommensurate transition [16, 27]. For such an effective theory,

the single particle wavefunction is $\exp(\mathrm{i}kx - \varepsilon t)$ where t is the imaginary time. Now we consider the effect of rotation in the x–t plane. Such a transformation is not covered in the Schrödinger group [28] but makes sense in the context of lattice models. When the coordinates are rotated by an angle θ, in order for the wavefunction to remain invariant, the dispersion relation of the rotated system must change to $\varepsilon' = \mathrm{i}k' \tan\theta + A(\cos\theta)^{-3}k'^2 + \mathrm{O}(k'^3)$ when $\theta \neq \pm\pi/2$ but to $\varepsilon' = \sqrt{\pm\mathrm{i}k'/A}$ when $\theta = \pm\pi/2$. Since the lattice model at $H = H_c$ and $V = 0$ is obtained by rotating that at $H = 0$ and $V = V_c$ by $\pi/2$, one naturally has excitations with $\sqrt{\mathrm{i}k'}$ dispersion at the $V = 0$ phase boundary. From this, we can interpret the $N^{-1/2}$ scaling at $H = H_c$ and $V = 0$ as the feature arising from viewing the ordinary PT transition with the spacetime coordinate interchanged. However, the anomalies c_1 and c_2 in the rotated system are not explained by such a simple effective theory.

Acknowledgments

The author thanks V Rittenberg, G v Gehlen and G Albertini for stimulating and helpful discussions and hospitality during his visit to Bonn University where this work was initiated. He also thanks J D Noh, V Popkov and H Lee for discussions and comments. This work was supported by Korea Science and Engineering Foundation through the Center for Theoretical Physics, Seoul National University, by Ministry of Education grant BSRI 96-2420 and by SNU Daewoo Research Fund.

Appendix A. Resursion relation of $J_\pm$

To show the recursion relation (21), we introduce an auxiliary function defined for $\Re y > 0$ as

$$\tilde{J}(y) = \frac{1}{2\mathrm{i}} \int_0^\infty \frac{\sqrt{y+\mathrm{i}t} - \sqrt{y-\mathrm{i}t}}{\mathrm{e}^{\pi t} - 1}\,\mathrm{d}t - \frac{1}{2}y^{1/2} + \frac{1}{3}y^{3/2}. \tag{A.1}$$

$\tilde{J}(y)$ is related to $J_\pm(y)$ by $J_+(y) = \sqrt{-\mathrm{i}}\tilde{J}(-\mathrm{i}y)$ for $\Im y > 0$ and $J_-(y) = \sqrt{\mathrm{i}}\tilde{J}(\mathrm{i}y)$ for $\Im y < 0$. Equation (21) follows from the recursion relation for $\tilde{J}(y)$ which is

$$\tilde{J}(y+2) = \tilde{J}(y) + \sqrt{y} \tag{A.2}$$

for $\Re y > 0$. To show (A.2), we employ the general sum formula [29]

$$\sum_{j=0}^{n} f(j) = \int_0^n f(x)\mathrm{d}x + \frac{f(n)+f(0)}{2} + 2\int_0^\infty \frac{\tilde{f}(n,t) - \tilde{f}(0,t)}{\mathrm{e}^{2\pi t} - 1}\,\mathrm{d}t \tag{A.3}$$

where $\tilde{f}(x,t) = (f(x+\mathrm{i}t) - f(x-\mathrm{i}t))/2\mathrm{i}$. This formula is valid if $f(x)$ is analytic and satisfies $\lim_{t\to\pm\infty} \mathrm{e}^{-2\pi|t|} f(x+\mathrm{i}t) = 0$ in the strip $-\delta < \Re x < n + \delta$ for some $\delta > 0$. Applying (A.3) to a trivial sum $\sum_{j=0}^{1} \sqrt{y+2j}$, one then obtains (A.2).

Appendix B. Partition function at $H = H_c$ and $V = 0$

In this appendix, we evaluate the partition function of the lattice model at the $V = 0$ phase boundary. That of the asymmetric XXZ chain follows simply redefining the nome and using the result of the lattice model for M even. For simplicity, we consider the case of M even and mention the other case at the end. Since M is even, from (46), we evaluate

$$\mathcal{Z}_F = \sum_{(r,m,\mathcal{P})} \exp(-\pi\sqrt{\tau}\,\mathcal{Y}_1^{(r,m,\mathcal{P})}) \tag{B.1}$$

where τ is given in (48).

First consider the case $(2r+m)$ even. Further, if m is in the range $-(2r+1) < m \leqslant (2r+1)$, $\mathcal{Y}_1^{(r,m,0)}$ is given in (42) and we have

$$\exp(-\pi\sqrt{\tau}\mathcal{Y}_1^{(r,m,0)}) = (\boldsymbol{q}\bar{\boldsymbol{q}})^{-c_1} \prod_{j=0}^{r-m/2-1} \bar{\boldsymbol{q}}^{\sqrt{1+2j}} \prod_{j=0}^{r+m/2-1} \boldsymbol{q}^{\sqrt{1+2j}} \tag{B.2}$$

where $\boldsymbol{q} = \exp(-\pi\sqrt{\mathrm{i}\tau})$ and $\bar{\boldsymbol{q}} = \exp(-\pi\sqrt{-\mathrm{i}\tau})$. From (30), one notes that $\exp(-\pi\sqrt{\tau}\mathcal{Y}_1^{(r,m,\mathcal{P})})$ is a product of $\exp(-\pi\sqrt{\tau}\mathcal{Y}_1^{(r,m,0)})$ and factors coming from particle and hole excitations. A particle at position p_k with $2p_k < (2r-m+1)$ contributes a factor of $\bar{\boldsymbol{q}}^{-\sqrt{1+2j}}$ where $j = r - m/2 - p_k = 0, 1, \ldots, (r-m/2-1)$, while that with $2p_k \geqslant (2r-m+1)$ a factor of $\boldsymbol{q}^{\sqrt{1+2j}}$ where $j = p_k - r + m/2 - 1 = 0, 1, \ldots, \infty$. A hole at h_k gives $\bar{\boldsymbol{q}}^{\sqrt{1+2j}}$ where $j = h_k + r - m/2 - 1 = r - m/2, r - m/2 + 1, \ldots, \infty$. Summing over all particle–hole configurations at the right end of the Fermi sea corresponds to evaluating a free fermion grand-canonical partition function under the constraint that the total number of particles should be the same as that of holes. If we denote the fugacity of each particle (hole) by z (z^{-1}), the desired sum is obtained by projecting out the z^0 term of the free fermion grand-canonical partition function which is

$$\Xi_1(z) = \prod_{j=0}^{r-m/2-1} (1 + z\bar{\boldsymbol{q}}^{-\sqrt{1+2j}}) \prod_{j=0}^{\infty} (1 + z\boldsymbol{q}^{\sqrt{1+2j}}) \prod_{j=r-m/2}^{\infty} (1 + z^{-1}\bar{\boldsymbol{q}}^{\sqrt{1+2j}}). \tag{B.3}$$

$\Xi_n(z)$ of this appendix and appendix D are not to be confused with $\Xi(b)$ defined in (13). We introduce a function $A(z)$ by

$$A(z) = \prod_{j=0}^{\infty} (1 + z\boldsymbol{q}^{\sqrt{1+2j}}) \prod_{j=0}^{\infty} (1 + z^{-1}\bar{\boldsymbol{q}}^{\sqrt{1+2j}}) \tag{B.4}$$

and denote its Fourier coefficients by A_n; $A(z) = \sum_n A_n z^n$. Then multiplying and dividing by a factor of $\prod_{j=0}^{r-m/2-1}(1 + z^{-1}\bar{\boldsymbol{q}}^{\sqrt{1+2j}})$ on the right-hand side of (B.3), we can put Ξ_1 in the form

$$\Xi_1(z) = z^{r-m/2} A(z) \prod_{j=0}^{r-m/2-1} \bar{\boldsymbol{q}}^{-\sqrt{1+2j}}. \tag{B.5}$$

Thus the coefficient of z^0 of $\Xi_1(z)$ is $A_{-r+m/2} \prod_{j=0}^{r-m/2-1} \bar{\boldsymbol{q}}^{-\sqrt{1+2j}}$. Note that the product over j in (B.5) is cancelled by that in (B.2). Summation over particle–hole configurations at the left end of the Fermi sea proceeds in exactly the same way with m replaced by $-m$ and $\boldsymbol{q}$ by $\bar{\boldsymbol{q}}$. Thus, the partition function after summation over all excitations from each m-shifted state is given as

$$\sum_{\mathcal{P}} \exp(-\pi\sqrt{\tau}\mathcal{Y}_1^{(r,m,\mathcal{P})}) = (\boldsymbol{q}\bar{\boldsymbol{q}})^{-c_1} A_{-r+m/2} \bar{A}_{-r-m/2} \tag{B.6}$$

for $-(2r+1) < m \leqslant (2r+1)$ where $\bar{A}_n$ stands for the complex conjugate of A_n. Similar calculations for each case of $m > (2r+1)$ and $m \leqslant -(2r+1)$ show that (B.6) holds for all m, provided $(2r+m)$ is even. We then sum the right-hand side of (B.6) over all even (odd) m's for $2r$ even (odd). However, we note that $\sum_m A_{-r+m/2}\bar{A}_{-r-m/2}$ is simply the coefficient of z^{-2r} in $|A(z)|^2$. To obtain the partition function in the $(2r+m)$ even sector, we finally sum over all integer (half-integer) values of r if N is even (odd). Even though the above derivations assumed $r \geqslant 0$, we may sum over negative r's by the symmetry, $|A(z)|^2 = |A(z^{-1})|^2$. Since the sum over r is equivalent to summing over all coefficients of even (odd) powers of z in $|A(z)|^2$, it can be written as $(A(1)^2 + A(-1)^2)/2$

$((A(1)^2 - A(-1)^2)/2)$ for N even (odd). Noting that $(q\bar{q})^{-c_1}A(1)^2/2 = \mathcal{Z}_1(q)$ and $(q\bar{q})^{-c_1}A(-1)^2/2 = \mathcal{Z}_2(q)$, we have the partition function in the $(2r+m)$ even sector as $\mathcal{Z}_1(q) \pm \mathcal{Z}_2(q)$ with $+$ $(-)$ sign for N even (odd).

Next consider the case of $(2r+m)$ odd. If m is in the range $-(2r+1) < m \leqslant (2r+1)$, $\mathcal{Y}_1^{(r,m,0)}$ is given in (43). Using the same method as above, we find the intermediate partition function as

$$\sum_{\mathcal{P}} \exp(-\pi\sqrt{\tau}\mathcal{Y}_1^{(r,m,\mathcal{P})}) = (q\bar{q})^{c_2} B_{-r+(m-1)/2}\bar{B}_{-r-(m+1)/2} \tag{B.7}$$

where B_n is defined through

$$B(z) = \prod_{j=1}^{\infty}(1 + zq^{\sqrt{2}j}) \prod_{j=0}^{\infty}(1 + z^{-1}\bar{q}^{\sqrt{2}j}) = \sum_n B_n z^n \tag{B.8}$$

and $\bar{B}_n$ is its complex conjugate. Similar calculations for each case of $m > (2r+1)$ and $m \leqslant -(2r+1)$ again show that (B.7) holds for all m, provided $(2r+m)$ is odd. Proceeding as above, we sum over m and r in (B.7) using the symmetry $z|B(z)|^2 = z^{-1}|B(z^{-1})|^2$ and finally find the partition function in $(2r+m)$ odd sector as $(q\bar{q})^{c_2}(B(1)^2 + B(-1)^2)/2$ for $2r$ odd and $(q\bar{q})^{c_2}(B(1)^2 - B(-1)^2)/2$ for $2r$ even. But $B(-1) = 0$ so that it becomes $(q\bar{q})^{c_2}B(1)^2/2 = \mathcal{Z}_3(q)$ for both parities of N. Adding this to that of $(2r+m)$ even sector, we have (49) for M even.

When M is odd, we need to insert a factor of $(-1)^m$ into (B.6) and (B.7). This does not complicate the sums since the sums over m in each sector are in steps of 2 and the sign factor is equivalent to $(-1)^{2r}$ for the case of (B.6) and $(-1)^{2r+1}$ for the case of (B.7). These extra sign factors then give the full partition function as given in (49) for M odd.

Appendix C. Spectra at $H = 0$ and $V = V_c$

In this section, we derive ΔE and ΔF at the phase boundary of $H = 0$. Although our main interest is for $H = 0$, discussions up to (C.11) and (C.12) hold for general $0 \leqslant H < H_c$.

When $|H| < H_c$, Z_∞ given by (11) has non-vanishing first derivative at $x_0 \equiv \exp(\pi\mathrm{i} + \lambda - b)$, the endpoint of the root distribution in bulk limit, which is related to H by (12). Thus, our starting ansatz for $Z_N^{-1}(x)$ is, instead of (17),

$$Z_N^{-1}(\pm\pi q + \pi\xi/N) = x_0^{\pm} + a_2\pi(y_\pm - \mathrm{i}\xi)/N + a_4\pi^2(y_\pm - \mathrm{i}\xi)^2/N^2 + \cdots \tag{C.1}$$

where $x_0^+ = x_0$ and $x_0^- = x_0\mathrm{e}^{-2\pi\mathrm{i}}$. Here, $y_\pm$, a_2 and a_4 are to be determined self-consistently. We then follow the same steps as in section 3. However, as we have seen in section 4, the levels not satisfying condition (36) become higher in energy by O(1) than those which do. This is because the roots of the Bethe ansatz equation, x_j or x_{Q-j}, for j finite, may not remain close to $x_0^{\pm}$. So, (C.1) is useful only to the levels which do satisfy (36). With the ansatz (C.1), the sum (18) is found to take the form

$$\begin{aligned} S[f] = \frac{N}{2\pi\mathrm{i}}\oint f(x)R_N(x)\frac{\mathrm{d}x}{x} + (m + \mathrm{i}y_+/2)f(x_0^+) - (m + \mathrm{i}y_-/2)f(x_0^-) \\ + f'(x_0)\Phi + f''(x_0)\Psi + \mathrm{O}(N^{-3}) \end{aligned} \tag{C.2}$$

where Φ and Ψ are short notations for

$$\Phi = a_2\pi Y_2(y_+, y_-)/N + a_4\pi^2 Y_4(y_+, y_-)/N^2 \tag{C.3}$$

$$\Psi = \tfrac{1}{2}a_2^2\pi^2 Y_4(y_+, y_-)/N^2 \tag{C.4}$$

with

$$Y_{2n}(y_+, y_-) = -\mathrm{i}J_+^{(n)}(y_+ + \mathrm{i} - 2m\mathrm{i}) + \mathrm{i}J_-^{(n)}(y_- - \mathrm{i} - 2m\mathrm{i}) + \sum_{k=1}^{n_+}\{[y_+ + \mathrm{i}(1 - 2m - 2p_k)]^n - [y_+ - \mathrm{i}(1 + 2m - 2h_k)]^n\} + \sum_{k=1}^{n_-}\{[y_- - \mathrm{i}(1 + 2m - 2\bar{p}_k)]^n - [y_- + \mathrm{i}(1 - 2m - 2\bar{h}_k)]^n\}. \tag{C.5}$$

Here, $J_\pm^{(n)}(y)$ are a generalization of (20):

$$J_\pm^{(n)}(y) = \frac{1}{2}\int_0^\infty \frac{(y+t)^n - (y-t)^n}{\mathrm{e}^{\pi t} - 1}\,\mathrm{d}t \pm \frac{\mathrm{i}}{2}y^n - \frac{1}{2(n+1)}y^{n+1}. \tag{C.6}$$

When $y_+ = y_-$ and $m = 0$, $(-1)^n Y_{2n}(y, y)$ reduces to $Y_{2n}(y)$ of I.

Using this general sum formula, we obtain the solution for R_N as

$$R_N(x) = R_\infty(x) + \frac{r}{N} + \frac{1}{N}\sum_{n\neq 0}\frac{\alpha^{|n|}}{1+\alpha^{|n|}}\left(\frac{x}{x_0}\right)^n \times \left(\frac{y_+ - y_-}{2\mathrm{i}} + \frac{n}{x_0}\Phi - \frac{n(n+1)}{x_0^2}\Psi\right) + \mathrm{O}(N^{-4}) \tag{C.7}$$

and the self-consistency equations for $y_\pm$, a_2 and a_4 as

$$y_\pm = (\pm 2r + m)\mathrm{i} + \pi^{-1}e_0(\Phi/x_0 - \Psi/x_0^2) + \mathrm{O}(N^{-3}) \tag{C.8}$$

$$-a_2^{-1} = \mathrm{i}Z'_\infty(x_0) + 2re_0x_0^{-1}N^{-1} + \mathrm{O}(N^{-3}) \tag{C.9}$$

$$2a_4a_2^{-3} = \mathrm{i}Z''_\infty(x_0) + \mathrm{O}(N^{-1}) \tag{C.10}$$

where $Z_\infty(x)$ is given in (11). Next, applying (C.2) with (C.7) and (C.8) to (3) and (5), we obtain after some algebra,

$$\Delta E = 2r(\Xi'(b) - V) + \Xi''(b)(x_0^{-1}\Phi - x_0^{-2}\Psi) - \Xi'''(b)x_0^{-2}\Psi + \mathrm{O}(N^{-3}) \tag{C.11}$$

for the chain and

$$\Delta F = -\pi\mathrm{i}m + 2r(\Xi(\lambda - b) - V) - \Xi'(\lambda - b)(x_0^{-1}\Phi - x_0^{-2}\Psi) - \Xi''(\lambda - b)x_0^{-2}\Psi + \mathrm{O}(N^{-3}) \tag{C.12}$$

for the lattice model where $\Xi(b)$ is defined in (13). The O(1) terms in (C.11) and (C.12) imply that the critical field V_c as a function of H is given by $\Xi'(b)$ for the chain and by $\Xi(\lambda - b)$ for the lattice. These O(1) terms vanish when $V = V_c$. Equations (C.11) and (C.12) contain, through Φ, an $\mathrm{O}(N^{-1})$ term proportional to $Y_2(y_\pm = \pm 2r\mathrm{i} + m\mathrm{i})$ which is purely imaginary. Thus the real parts of the energy gaps at the antiferromagnetic phase boundary are $\mathrm{O}(N^{-2})$.

Up to here H has been general. For simplicity, we now specialize to $H = 0$ at corresponding values of the critical vertical field. When $H = 0$, $x_0 = -\mathrm{e}^\lambda$, $b = 0$ and $a_2 = \mathrm{e}^\lambda/e_2 + \mathrm{O}(N^{-1})$. Setting $b = 0$ in (C.11) and (C.12), one notes that the imaginary $\mathrm{O}(N^{-1})$ terms all vanish simplifying the results considerably. A final expression for ΔE and ΔF then becomes as given in (57) and (55), respectively, where $\mathcal{Y}_4^{(r,m,\mathcal{P})}$ is the value of $Y_4(y_+, y_-)$ evaluated at the zeroth-order solution for $y_\pm$, i.e. $Y_4(y_\pm = \mathrm{i}(\pm 2r + m))$.

Appendix D. Partition functions at $H = 0$ and $V = V_c$

In this appendix, we derive (60). Consider the lattice model on the $M \times N$ lattice with M and N even. Then from (58) and (59), we have

$$\mathcal{Z}_F = \sum_{(r,m,\mathcal{P})} \boldsymbol{p}^{\mathcal{Y}_4^{(r,m,\mathcal{P})}} \tag{D.1}$$

with $\mathcal{Y}_4^{(r,m,\mathcal{P})}$ given in (56) and the sum is for $r = 0, 1, \ldots$ under restriction (36). Considering first $(2r + m)$ even sector, from (56), one sees that a particle (hole) at position p_k (h_k) contributes $\boldsymbol{p}^{-(1+2j)^2}$ ($\boldsymbol{p}^{(1+2j)^2}$) with $0 \leqslant j \leqslant r - m/2 - 1$ ($j \geqslant r - m/2$). Thus, the free fermion grand-canonical partition function for the right-hand side excitation is

$$\Xi_3(z) = \prod_{j=0}^{r-m/2-1} (1 + z\boldsymbol{p}^{-(1+2j)^2}) \prod_{j=r-m/2}^{\infty} (1 + z^{-1}\boldsymbol{p}^{(1+2j)^2}) = z^{r-m/2} C(z) \prod_{j=0}^{r-m/2-1} \boldsymbol{p}^{-(1+2j)^2} \tag{D.2}$$

where

$$C(z) = \prod_{j=0}^{\infty} (1 + z^{-1}\boldsymbol{p}^{(1+2j)^2}) = \sum_{n=0}^{\infty} C_n z^{-n}. \tag{D.3}$$

Thus the coefficient of z^0 in $\Xi_3(z)$ can be written as $C_{r-m/2} \prod_{j=0}^{r-m/2-1} \boldsymbol{p}^{-(1+2j)^2}$. The left-hand side excitations give the same result with $m \to -m$. Using the fact that $\sum_{j=0}^{r-m/2-1}(1+2j)^2 + \sum_{j=0}^{r+m/2-1}(1+2j)^2 = 8r^3/3 - 2r/3 + 2rm^2$, we note that the product in the second line of (D.2) is cancelled by that coming from the first terms of $\mathcal{Y}_4^{(r,m,\mathcal{P})}$. Thus we have

$$\sum_{\mathcal{P}} \boldsymbol{p}^{\mathcal{Y}_4^{(r,m,\mathcal{P})}} = C_{r-m/2} C_{r+m/2}. \tag{D.4}$$

Summing (D.4) over m from $-2r$ to $+2r$ in steps of 2 and over $r \geqslant 0$, we find the partition function in the $(2r + m)$ even sector as $(C(1)^2 + C(-1)^2)/2 = \tilde{\mathcal{Z}}_1(\boldsymbol{p}) + \tilde{\mathcal{Z}}_3(\boldsymbol{p})$.

Next consider the $(2r + m)$ odd sector. In this case the free fermion grand-canonical partition function for the right-hand side excitations is

$$\Xi_4(z) = \prod_{j=0}^{r-(m+1)/2} (1 + z\boldsymbol{p}^{-4j^2}) \prod_{j=r-(m-1)/2}^{\infty} (1 + z^{-1}\boldsymbol{p}^{4j^2}) \tag{D.5}$$

while that for the left-hand side is

$$\tilde{\Xi}_4(z) = \prod_{j=1}^{r+(m-1)/2} (1 + z\boldsymbol{p}^{-4j^2}) \prod_{j=r+(m+1)/2}^{\infty} (1 + z^{-1}\boldsymbol{p}^{4j^2}). \tag{D.6}$$

Note that the $j = 0$ term is excluded in (D.6) due to the strict inequality in (36). Defining

$$D(z) = \prod_{j=0}^{\infty} (1 + z^{-1}\boldsymbol{p}^{4j^2}) = \sum_{n=0}^{\infty} D_n z^{-n} \tag{D.7}$$

$$\tilde{D}(z) = \prod_{j=1}^{\infty} (1 + z^{-1}\boldsymbol{p}^{4j^2}) = \sum_{n=0}^{\infty} \tilde{D}_n z^{-n} \tag{D.8}$$

we can write

$$\sum_{\mathcal{P}} \boldsymbol{p}^{\mathcal{Y}_4^{(r,m,\mathcal{P})}} = D_{r-(m-1)/2} \tilde{D}_{r+(m-1)/2} \tag{D.9}$$

where $\sum_{j=0}^{r-m/2-1/2}(2j)^2+\sum_{j=1}^{r+m/2-1/2}(2j)^2 = 8r^3/3-2r/3+2rm^2$ has been used. We then sum (D.9) over m from $-2r+1$ to $2r+1$ in steps of 2 and finally over $r \geqslant 0$ to obtain the remaining piece of the partition function as $(D(1)\tilde{D}(1) + D(-1)\tilde{D}(-1))/2 = \tilde{\mathcal{Z}}_2(\boldsymbol{p})$. We thus arrive at (60) for M and N even. For other parities of M and N, we repeat the above steps with only minor changes and find (60).

References

[1] Albertini G, Dahmen S R and Wehefritz B 1996 *J. Phys. A: Math. Gen.* **29** L369
[2] Albertini G, Dahmen S R and Wehefritz B 1996 *Preprint* cond-mat/9606137
[3] Noh J D and Kim D 1996 *Phys. Rev.* E **53** 3225
[4] Gwa L H and Spohn H 1992 *Phys. Rev.* A **46** 844
Gwa L H and Spohn H 1987 *Phys. Rev. Lett.* **68** 725
[5] Neergaard J and den Nijs M 1995 *Phys. Rev. Lett.* **74** 730
[6] Kim D 1995 *Phys. Rev.* E **52** 3512
[7] Baxter R J 1982 *Exactly Solvable Models in Statistical Mechanics* (London: Academic)
[8] Lieb E H and Wu F Y 1972 *Phase Transitions and Critical Phenomena* vol 1, ed C Domb and M S Green (London: Academic)
[9] Gaudin M 1983 *La Fonction d'Onde de Bethe* (Paris: Masson)
[10] Nolden I M 1992 *J. Stat. Phys.* **67** 155
[11] van Beijeren H 1977 *Phys. Rev. Lett.* **38** 993
[12] Jayaprakash C, Saam W F and Teitel S 1983 *Phys. Rev. Lett.* **50** 2017
[13] Bukman D J and Shore J D 1995 *J. Stat. Phys.* **78** 1277
[14] Akutsu Y, Akutsu N and Yamamoto T 1988 *Phys. Rev. Lett.* **61** 424
[15] Pokrovsky V L and Talapov A L 1980 *Zh. Eksp. Teor. Fiz.* **78** 269
Pokrovsky V L and Talapov A L 1980 *Sov. Phys.–JETP* **51** 134
[16] den Nijs M 1988 *Phase Transitions and Critical Phenomena* vol 12, ed C Domb and J L Lebowitz (London: Academic)
[17] Privman V 1990 *Finite Size Scaling and Numerical Simulation of Statistical Systems* (Singapore: World Scientific)
[18] Ginsparg P 1988 *Nucl. Phys.* B **295** 153
[19] Plischke M, Rácz Z and Liu D 1987 *Phys. Rev.* B **35** 3485
[20] Kardar M, Parisi G and Zhang Y C 1986 *Phys. Rev. Lett.* **56** 889
[21] Henkel M and Schütz G 1994 *Physica* **206A** 187
[22] Derrida B, Evans M R and Mukamel D 1993 *J. Phys. A: Math. Gen.* **26** 4911
[23] Dhar D 1987 *Phase Transitions* **9** 51
[24] Sutherland B, Yang C N and Yang C P 1967 *Phys. Rev. Lett.* **19** 588
[25] Baxter R J 1973 *J. Stat. Phys.* **9** 145
[26] Wehefritz B and Dahmen S R 1996 Private communication
[27] Noh J D and Kim D 1994 *Phys. Rev.* E **49** 1943
[28] Henkel M 1994 *J. Stat. Phys.* **75** 1023
Henkel M 1996 *Preprint* cond-mat/9610174
[29] Dieudonné J 1971 *Infinitesimal Calculus* (Paris: Hermann) p 285